Biology of Reproduction, 2023, 1–12
https://doi.org/10.1093/biolre/ioad133
Research Article

The effects of heat stress on intrauterine development, reproductive function, and ovarian gene expression of F1 female mice as well as gene expression of F2 embryos†

José R. Silva[1], Joanna M. G. Souza-Fabjan[1,2], Tays F. M. Bento[1], José R. Silva[3], Cristiane R. F. Moura[3], Pawel M. Bartlewski[4] and Ribrio I. T. P. Batista[1,2,*]

[1]Programa de Pós-Graduação em Ciência e Biotecnologia, Universidade Federal Fluminense, Niterói, RJ, Brazil
[2]Faculdade de Veterinária, Universidade Federal Fluminense, Niterói, RJ, Brazil
[3]Departamento de Ciências Básicas, Universidade Federal dos Vales do Jequitinhonha e Mucuri, Diamantina, MG, Brazil
[4]Department of Biomedical Sciences, Ontario Veterinary College, University of Guelph, Guelph, ON, Canada
***Correspondence**: Programa de Pós-Graduação em Ciência e Biotecnologia (PPBI), Universidade Federal Fluminense, Rua Professor Marcos Waldemar de Freitas Reis, Bloco M, sala 229C São Domingos, Niterói, RJ, CEP 24210-201, Brazil. Tel: +55 32 99166 5479; E-mail: ribrio@yahoo.com.br

†**Grant Support**: This work was supported by Fundação de Amparo à Pesquisa do Estado do Rio de Janeiro (FAPERJ). The funder was not involved in the design of the study, in the collection, analysis, or interpretation of data, in the writing of the manuscript, or in the decision to publish the results.

Abstract

Exposure to heat stress (HS) in utero was postulated to trigger an adaptive molecular response that can be transmitted to the next generation. Hence, this study assessed the impact of HS exposure at different stages of the gestational period of mice on the female F1 population and their offspring. Heat stress exposure (41°C and 65% relative humidity—RH) occurred during the first half (FP), the second half (SP), or the entire pregnancy (TP). A control group (C) was maintained in normothermic conditions (25°C, 45% RH) throughout the experiment. Heat stress had a significant negative effect on intrauterine development, mainly when HS exposure occurred in the first half of pregnancy (FP and TP groups). Postnatal growth of FP and TP mice was hindered until 4 weeks of age. The total number of follicles per ovary did not vary ($P > 0.05$) between the control and HS-exposed groups. Mean numbers of primordial follicles were lower ($P < 0.05$) in the sexually mature FP than those in SP and TP F1 females. However, the mean number of viable embryos after superovulation was lower ($P < 0.05$) in TP compared with C group. The expression of genes associated with physiological and cellular response to HS, autophagy, and apoptosis was significantly affected in the ovarian tissue of F1 females and F2 in vivo-derived blastocysts in all HS-exposed groups. In conclusion, exposure to HS during pregnancy compromised somatic development and reproductive parameters as well as altered gene expression profile that was then transmitted to the next generation of mice.

Graphical Abstract

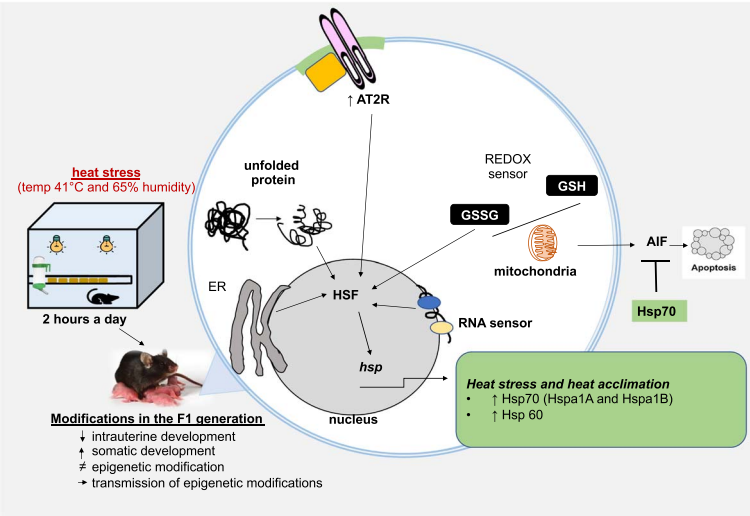

Keywords: climate change, embryonic development, prenatal programming, epigenetic, postnatal period, mouse

Received: May 12, 2023. **Revised:** August 30, 2023. **Accepted:** October 1, 2023

Introduction

Global climate change is associated with increased frequency, intensity, and duration of extreme weather conditions, putting at risk the existence of life-sustaining ecosystems. During 2021 and 2022, atypical weather events caused devastations on every continent, with fatal floods and forest fires in several countries [1] that resulted in human and animal deaths and billions of dollars in economic losses. Recent climate changes have been associated with an increase in the average global temperature as well as the frequency and duration of heat waves, resulting in all-time record temperatures in several countries including Australia, Canada, India, Italy, Oman, Turkey, Pakistan, and the United Kingdom [1–3]. Extreme heat contributes to drought conditions [2], which in turn leads to food shortages and increased incidence of insect-borne diseases [3]. Exposure to high ambient temperatures causes acute respiratory and cardiovascular disorders [4]. In 2003, heat waves in Europe caused more than 70 000 deaths, usually attributed to heat stress (HS)-induced respiratory/cardiovascular shock and/or exacerbation of various comorbidities [5].

Heat stress is defined as an inability of the organism to sufficiently dissipate heat and maintain optimal temperature, culminating in hyperthermia [6, 7]. Normally, animals and human beings respond to HS by redirecting blood flow to the skin (vasodilation) to increase heat transfer to the external environment and by sweating [8]. These physiological responses to HS are necessary to counter any increases in core body temperature; however, sweat production can lead to dehydration if the resulting body water deficits are not adequately replenished. Dehydration decreases circulating blood volume, presaging cardiovascular strain [9] and potential kidney injury and/or failure [10, 11]. The renin–angiotensin system (RAS), involving sequential proteolysis of the angiotensinogen precursor in blood plasma, plays an important role in the development of hypertension and regulation of water/mineral homeostasis [12]. There is a great deal of evidence to suggest that HS activates RAS, which also entails angiotensin II (Ang II) binding to G protein-coupled receptors AT1R and AT2R [13, 14]. Both these receptors not only mediate the control of systemic hemodynamics and blood volume, but also govern the stimulation of cell proliferation and differentiation, or tissue remodeling, in stressful situations.

At the cellular level, HS may exert deleterious effects on (i) DNA/RNA synthesis and processing, (ii) cell cycle progression, (iii) protein configuration and stability, (iv) cytoskeletal components, (v) ATP synthesis, and (vi) membrane permeability (leading to an increase in intracellular Na^+, H^+, and Ca^{2+} content) [15]. The ability to adapt to HS appears to be an intrinsic cell function as cellular stress responses are ubiquitous among eukaryotes and prokaryotes [16]. Such an ability to mount an appropriate compensatory stress response [17] can be epigenetically transmitted to future generations [18]. A compensatory response is a highly conserved cascade of altered gene expression and protein activation processes [17], with a family of transcription factors known as heat shock factors playing a critical role during the rise in cellular temperature [19, 20]. These factors coordinate the cellular response to HS by altering the expression of a wide variety of genes, including heat shock proteins (HSPs) [21]. There are several HSP families that are classified according to their molecular weight: HSP110, HSP90, HSP70, HSP60, and small HSPs such as HSP27 and ubiquitin [22]. Heat shock proteins play a central cytoprotective role during HS by preventing cell death and tissue injury [23, 24]. Interestingly, Ang II has been shown to induce HSP expression in vitro [25].

In addition to the role of HSPs, the response to HS also involves autophagy that degrades and recycles damaged organelles in lysosomes [26]. The heat shock factor-1 enhances the expression of autophagy genes, which participate in generating a protective response and extend cellular lifespan [27]. In stressful situations, mitochondria and endoplasmic reticulum can trigger the unfolded protein response (UPR), which promotes the functional recovery of these organelles [28]. However, when the stressors are persistent and the UPR is not sufficient to deal with resultant dysfunctions, the elimination of organelles by autophagy can occur [29]. Autophagy is a genetically programmed and evolutionarily conserved catabolic process that degrades damaged or excess cellular proteins and organelles through the formation of a double-membrane structure known as an autophagosome. Autophagosome assembly involves the activation of ATG-5 [30] and ATG-8 [31], commonly used as markers of the autophagic pathway.

Pregnant women are particularly sensitive to HS. They are at a high risk of suffering from heat-related disorders including heat stroke, respiratory conditions, and birthing complications [32, 33]. There is a growing body of literature on animals [34] and humans [35, 36] suggesting that HS during the gestational period is a potential teratogen. In livestock species, gestational HS reduces both the productive and reproductive capacity of animals; in addition to adverse effects on embryonic development, it promotes epigenetic changes that can be transmitted to future generations [18]. In humans, numerous systematic reviews have associated HS with preterm delivery, low birth weight, and abortions [37–39]. Proper interpretation of HS-allied pathologies is confounded by variability in the "windows of exposure" (e.g., intermittent or continued exposure to heat during pregnancy) and inconsistencies in defining what constitutes excess heat. As a result, more studies are urgently needed to expand our current knowledge of HS and develop effective preventive methods.

Therefore, in the present study, we used mice as a biological model to assess the impact of HS at different gestational periods on the pregnancy rate, prolificacy, and birth weight of pups. In addition, females of the F1 generation were evaluated for somatic development, ovarian follicular populations, and responsiveness to hormonal superovulation. Finally, the cellular response to HS and the transmission of this response to the F2 generation of mice were examined by analyzing the expression of select genes in the ovarian tissue (F1 females) and F2 embryos, respectively. For this, we selected genes involved in the (i) physiological (*AT1R* and *AT2R*) and cellular response to HS (*HSPA1A*; *HSPA1B*; *HSP40*; *HSP60*; *HSP90AAI*; *HSP90ABI*), and (ii) elimination of macromolecules and organelles damaged by autophagy (*ATG5* and *ATG8*) and programmed cell death (*BAX*, *BCL-2*, *CASP3*, and *CASP9*). The transmission capacity of the HS response was inferred by analyzing the expression of some differentially expressed genes in the F2 embryo, in addition to the genes associated with embryonic competence (*CDX2* and *OCT-4*).

Materials and methods

The present study was approved by the Animal Use Ethics Committee (CEUA), under protocol number 003/2018, of the Federal University of the Jequitinhonha and Mucuri Valleys, in Diamantina, Minas Gerais state, Brazil.

Animals and general experimental design

Forty female C5BL/6J mice, aged 5–6 weeks, were mated with 40 males of the same age and strain in a 1:1 ratio (Figure 1). Detection of the vaginal plug (day 1) was done to confirm the successful mating. Subsequently, the females were subjected to HS during the first (FP, from days 1 to 10; $n = 10$) or second half of gestation (SP, from day 11 to delivery; $n = 10$), or throughout the entire duration of pregnancy (TP, $n = 10$). A control group (C, $n = 10$) was maintained in normothermic conditions (25°C, 45% relative humidity) throughout the present experiment. After delivery, the birthweight of offspring was recorded and the somatic development of F1 females was monitored weekly until 8 weeks of age. At 8 weeks, 10 females from each group were superovulated and mated with control F1 males in the four configurations: FP × C, SP × C, TP × C, and C × C; females and males, respectively. The females were euthanized by cervical dislocation 72 h after mating; uterine lavage was performed, and all the recovered structures were examined for viability and developmental stage. One ovary from each superovulated female was collected and fixed for histological analysis, while the other was frozen for gene expression analysis. The embryos from superovulated females that attained a blastocyst stage were also frozen for ensuing gene expression analysis.

Heat stress induction

Heat stress induction during the gestational period was performed daily for 2 h (1:00 p.m. to 3:00 p.m.), starting 6 h after the beginning of the light cycle, according to the method previously described by Aroyo et al. [40]. A standard cage with the mice was placed inside an environmental chamber (70 × 80 × 50 cm) with a 4-mm-thick transparent acrylic top and two doors for frontal access. The chamber was heated by two Siccatherm red lamps (SICCATHERM-RED; OSRAM, Shanghai, China) so that the mice were not exposed to radiative heat. A container filled with water (500 mL) was kept inside the chamber to generate the required humidity. Temperature and humidity (41°C, 65% humidity) inside the chamber were monitored by an automated digital thermometer hygrometer humidity meter (UNI-T UT 330B digital USB; Beijing, China). During the entire HS induction period, the animals had unrestricted access to commercial feed (Nuvilab Cr-1; Nuvital Nutrientes S/A, São Paulo, Brazil) and drinking water. The control group was subjected to the same movement and confinement conditions.

Monitoring somatic development of the progeny

The mean number of live newborn pups per female was recorded at parturition. Subsequently, the litters were monitored weekly for somatic development, by weighing each pup on an analytical digital scale (Ohaus PX124/E AM—Pioneer Analytical Balance, 0.0001 g resolution, Parsippany, NJ, USA). Combined data from animals of both sexes were recorded and analyzed up to the age of 3 weeks, when sexing was performed. From the third to the eighth week of age, only the data from females were collated [41]. This was done to avoid errors in animal sexing since stress during pregnancy induces demasculinization, characterized by shortening of the anogenital distance in male offspring [42].

Superovulation and embryo collection

Females were superovulated by intraperitoneal administration of 5 IU of equine chorionic gonadotropin (Folligon; Intervet, São Paulo, SP, Brazil), followed by an injection of 5 IU of human chorionic gonadotropin (hCG; Chorulon, Intervet) 48 h later; both gonadotropin preparations were diluted in 0.1 mL of sterile saline solution [41]. Following the hCG treatment, females were mated overnight. At 72 h after mating, the females were sacrificed, and their reproductive tracts were removed. Both uterine horns were perfused with 0.5 mL of phosphate-buffered saline (PBS) containing 0.4% of bovine serum albumin. The recovered perfusion medium was placed in Petri dishes and the embryos were identified using a stereomicroscope (Olympus SZ-1145, Tokyo, Japan). All identified structures were classified according to the development stage (unfertilized, cleaved (2–8), morula, compact morula, early blastocyst, blastocyst, and expanded blastocyst) and quality (presence or absence of cell extrusion and fragmentation).

Ovarian histology and follicle quantification

Quantification of ovarian follicles was performed according to the methodology described by Campos-Junior et al. [43]. Briefly, every third cryotome section (5 μm) was used to classify and count ovarian follicles. The follicles were classified as follows: (i) primordial follicles (the oocyte surrounded by a single layer of flattened granulosa cells); (ii) primary follicles (follicles with a single layer of cuboidal cells around the oocyte); (iii) secondary follicles (follicles with two layers of cuboidal cells around the oocyte); (iv) tertiary (antral) follicles with an apparent follicular antrum. The final number of follicles in each category was determined on a per-ovary basis using the following formula developed by Gougeon and Chainy [44]:

$$FP = \frac{NF \times NS \times HC}{NSA \times ADON}$$

where FP = follicular population, NF = total number of follicles in the ovary (primordial, primary, secondary, and tertiary), NS = number of sections per ovary, HC = histological section thickness, NSA = number of sections analyzed, and $ADON$ = average diameter of the oocyte nucleus (primordial, primary, secondary, and tertiary). The estimation of the follicular recruitment (activation) rate was carried out as previously described by Campos-Junior et al. [43], using the following formula:

$$FAT = \frac{FP + SF + AF}{TF} \times 100$$

where FAT = follicular activation rate, FP = primary follicle number, SF = secondary follicle number, AF = antral follicle number, and TF = total follicle number.

Gene expression

For gene expression analysis, 20 ovaries and 100 blastocysts obtained from 20 animals were used ($n = 5$ animals per group). After collection, five embryos at the blastocyst stage recovered from each animal were grouped to form a pool. Then, the pool was washed three times in PBS supplemented with 0.1% of polyvinyl alcohol and frozen in liquid nitrogen

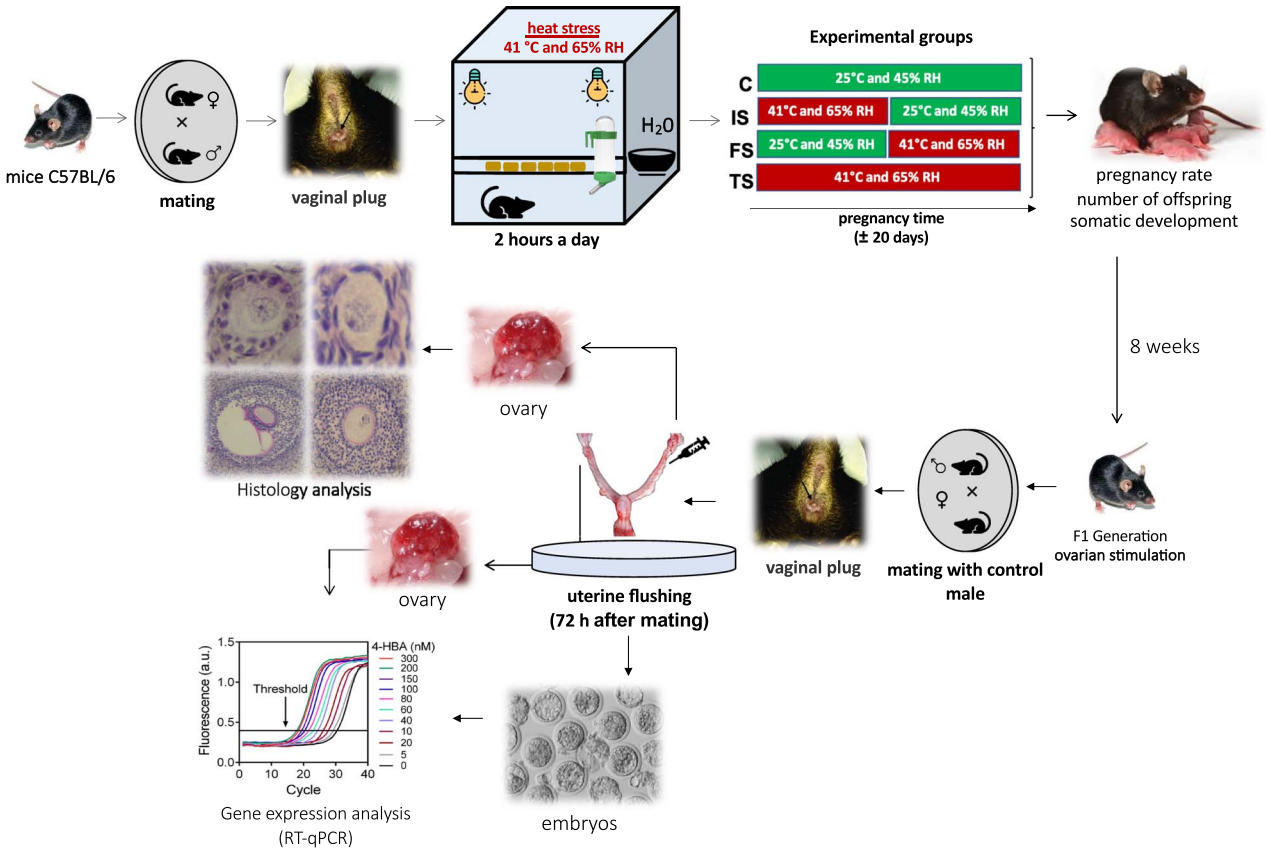

Figure 1. Experimental design. Forty female C5BL/6J mice, aged 5–6 weeks, were mated with 40 males of the same age and strain in a 1:1 ratio. After vaginal plug detection (day 1), the females were subjected to HS (41°C, 65% relative humidity—RH) during the first (FP, from days 1 to 10; $n = 10$) or second half of gestation (SP, from day 11 to delivery; $n = 10$), or throughout the entire duration of pregnancy (TP, $n = 10$). A control group (C, $n = 10$) was maintained in normothermic conditions (25°C, 45% RH) throughout the present experiment. After delivery, the birthweight of offspring was recorded and the somatic development of F1 females was monitored weekly until 8 weeks of age. At 8 weeks, 10 females from each group were superovulated and mated with control F1 males in the four configurations: FP × C, SP × C, TP × C, and C × C; females and males, respectively. Uterine lavage was performed 72 h after confirmed mating and all the recovered structures were examined for viability and developmental stage. One ovary from each superovulated female was collected and fixed for histological analysis, while the other was frozen for gene expression analysis. The embryos from superovulated females that attained a blastocyst stage were also frozen for ensuing gene expression analysis.

using DNase- and RNase-free cryotubes (Corning, NY, USA). Adipose tissue-free ovaries were also washed and frozen as described for embryo pools above.

Total RNA isolation and reverse transcription

Total RNA isolation was performed using an RNeasyMicro Kit (Qiagen Inc., Valencia, CA, USA) according to the manufacturer's instructions and with the DNase pretreatment for 15 min to avoid DNA contamination. RNase-free water (14 μL) was added, and RNA quantification of each sample (1 μL) was performed using a spectrophotometer (Nanodrop 2000, Wilmington, DE, USA). The SuperScript III first-strand synthesis Supermix (Invitrogen, Carlsbad, CA, USA) was used for reverse transcription, and the same RNA concentration (0.05 and 1.0 μg per embryo and ovary sample) was used in all samples. A mixture of oligo (dT) 20 primers, dNTP mixture, Superscript III-RT, RNase OUT, $MgCl_2$, RT buffer, and RNA sample in a final volume of 20 μL was incubated at 65°C for 5 min and then at 50°C for 50 min. The reaction was terminated at 85°C (5 min) and then the samples were chilled on ice. Following these steps, the samples were incubated with RNase H to degrade the RNA strand of any RNA–DNA hybrids according to the manufacturer's instructions. The cDNA was then stored at −20°C until use at a later date.

Quantitative RT-qPCR amplification

The relative mRNA quantification was done using real-time quantitative polymerase chain reaction (RT-qPCR; QuantStudio 3 Real-Time PCR Systems, Applied Biosystems Thermo Fisher Scientific, Wilmington, DE, USA), in triplicate. The qPCR reactions (20 μL of total volume) were conducted with a mixture of SYBR green kit (10 μL; Power SYBR Green, Applied Biosystems), 0.1 μM of primers (1 μL; described in Table 1), nuclease-free water (8.5 μL), and reverse transcribed cDNA (0.5 μL). Negative controls were similarly run with each group of samples containing the RT-qPCR reaction mixture without nucleic acids. Thermal cycling was composed of an initial denaturation step at 95°C for 10 min followed by 45 cycles of denaturation at 95°C for 15 s, primer annealing (Table 1) for 15 s, and extension at 72°C for 30 s. Fluorescence data were acquired during the extension steps. Afterwards, the dissociation curve was obtained by melting the amplicon from 60 to 95°C to confirm that a single specific product was generated. Primer efficiency was calculated using the LinRegPCR software. The expression of the specific gene was normalized against the geometric mean expression of three housekeeping genes: actin beta (β-actin), glyceraldehyde-3-phosphate dehydrogenase (*GAPDH*), and H2A histone family, member Z (*H2AFZ*). The stability (smaller variation due to

Table 1. RT-qPCR primer sequences and annealing temperatures.

Gene	Primer sequences 5′ to 3′	Annealing temperature (°C)	References
ATG5	F: GGAGAGAAGAGGAGCCAGGT R: TGTTGCCTCCACTGAACTTG	55	[31]
ATG8	F: TTCTTCCTCCTGGTGAATGG R: GTGGGTGCCTACGTTCTCAT	55	[31]
BAX	F: ATGCGTCCACCAAGAAGCTGAG R: CCCCAGTTGAAGTTGCCATCAG	60	[46]
BCL-2	F: GTCGCTACCGTCGTGACTTC R: CAGACATGCACCTACCCA	60	[47]
CDX-2	F: AATCAAGAAGAAGCAGCAGCAG R: GTCCATACTCCTCATGGCTCA	60	[31]
CASP3	F: ATGGGAGCAAGTCAGTGGAC R: CGTACCAGAGCGAGATGACA	60	[31]
CASP9	F: TCCTGGTACATCGAGACCTTG R: AAGTCCCTTTCGCAGAAACAG	63	[48]
HSP 40	F: AGGCATGGACATTGATGACACA R: CCACCCATACCCATTGGAAAG	60	[49]
HSP 60	F: CATCGGAAGCCATTGGTCATAA R: CGTGCTTAGAGCTTCTCCGTCA	60	[49]
HSPA1A	F: AGACTGTTGAGTTCTTTGTGTTTGGA R: GAAGGACCCGACACAAGCAT	60	[50]
HSPA1B	F: CCATCGAGGAGGTGGATTAGAG R: GAACCATGAAGAAGACTTTAAATAACC	60	[50]
HSP90AAI	F: ATGGAGAGAATCATGAAAGCTCAA R: TGCTGCCATGTAACCCATTG	60	[50]
HSP90ABI	F:TGGGAAAGAGCTGAAAATTGACAT R:TGCCTGTGTCCACCAAAGTC	60	[50]
NANOG	F: CACAGTTTGCCTAGTTCTGAGG R: GCAAGAATAGTTCTCGGGATGAA	60	[51]
OCT-4	F: CGGAAGAGAAAGCGAACTAGC R: ATTGGCGATGTGAGTGATCTG	60	[48]
B-ACTIN	F: GCTCTGGCTCCTAGCACCAT R: GCCACCGATCCACACAGAGT	60	[52]
GAPDH	F: CTCCCACTCTTCCACCTTCG R: GCCTCTCTTGCTCAGTGTCC	60	[53]
H2AFZ	F: TAGGACAACCAGCCACGGA R: GATGACACCACCACCAGCAA	60	[53]
AT1R	F: CTTTTCTGGGTTGAGTTGGTCT R: GGCTGGCATTTTGTCTGGATA	60	[54]
AT2R	F: CAGCAACTCCAAATTCTTACACC R: AGCTTACTTCAGCCTGCATT	60	[54]

the treatment) of the reference genes was calculated according to the methodology described by Pfaffl et al. [45], using the BestKeeper—Excel tool. The values of the Pearson correlation coefficient observed for *β-actin* ($r^2 = 0.70$), *GAPDH* ($r^2 = 0.78$), and *H2AFZ* ($r^2 = 0.77$) genes were indicative of stability ($P < 0.01$) of these reference genes.

The ovarian tissue was evaluated for the abundance of transcripts associated with (i) autophagy (*ATG5* and *ATG8*), (ii) angiotensin II receptor (*AT1R* and *AT2R*), (iii) heat stress (*HSPA1A*, *HSPA1B*, *HSP40*, *HSP60*, *HSP90AAI*, and *HSP90ABI*), and (iv) apoptosis (*BAX*, *BCL-2CASP3*, and *CASP9*). The embryos were evaluated for transcripts associated with (i) embryo competence (*CDX2* and *OCT-4*), (ii) angiotensin II receptor (*AT2R*), (iii) heat stress (*HSPA1A* and *HSP90AAI*), and (iv) autophagy (*ATG8*).

Statistical analysis

Data were analyzed using the GraphPad Prism version 5.0 (GraphPad Software, San Diego, CA, USA). Pregnancy rates were analyzed using the chi-square test. Numbers and birth weight of pups, their ensuing somatic development, females' follicular populations, and follicular activation data were tested for normality using the Kolmogorov–Smirnov test before being submitted to one-way analysis of variance (ANOVA) followed by the Tukey HSD test. Superovulatory responses were analyzed using the Kruskal–Wallis test. After testing for normality using a Kolmogorov–Smirnov test, gene expression data were analyzed with the General Linear Model ANOVA, followed by Tukey post hoc. Differences were considered significant when the *P* value was <0.05.

Results

Pregnancy rate, prolificacy, and birth weight

Twenty-four pregnancies were confirmed in 40 females with a detected vaginal plug (60%) with a total of 163 pups born. There was no difference among the experimental groups ($P > 0.05$) in terms of pregnancy rates and mean numbers of offspring born (Table 2). However, all groups exposed to HS had lower mean birthweight than C group ($P < 0.0001$). When the comparison was performed only within the

Table 2. Pregnancy rates as well as mean (± SEM) numbers (per female) and birthweights of offspring in C57BL/6 mice submitted to heat shock at different stages of the gestational period.

Variables	C	FP	SP	TP
Pregnancy rate (%)	80 (8/10)	40 (4/10)	60 (6/10)	60 (6/10)
Duration of gestational period (days)	20.1 + 1.3	19.9 + 1.2	17.5 + 2.5	17.8 + 1.6
Number of offspring	7.0 ± 1.0	6.0 ± 1.5	6.5 ± 1.5	5.1 ± 1.5
Birthweight (g)	2.2 ± 0.1[a]	1.1 ± 0.2[c]	1.8 ± 0.1[b]	1.2 ± 0.1[c]

C: control—animals maintained under normothermic conditions; FP—animals exposed to heat stress daily for 2 h during the first half of pregnancy (days 1–10); SP—animals exposed to heat stress daily for 2 h during the second half of pregnancy (days 11 to parturition); TP: animals exposed to heat stress daily for 2 h throughout the entire gestational period. Different letter superscripts in the same column indicate significant differences between the groups ($P < 0.05$).

experimental groups, the HS produced a greater effect in the first than in the second half of pregnancy, reducing ($P < 0.05$) the average birth weight in FP and TP groups in comparison to SP group.

Somatic development

Postnatal somatic development was monitored in 155 of 163 offspring, of which 79 and 76 were sexed as males (50.9%) and females (49.1%), respectively, after the third week of life (Figure 2A). At the time of birth, the mean body weight was greater ($P < 0.05$) for SP than C group, and the pups in both groups had a greater ($P < 0.05$) mean body weight compared with those in FP and TP groups. At 2 weeks of age, the mean body weight was lowest ($P < 0.05$) in TP and it was greater for C compared with FP animals. Finally, at 1, 3, and 4 weeks post-partum, the mean body weight was greater ($P < 0.05$) for both C and SP mice than for FP and TP animals. From 3 weeks post-partum onwards, somatic development was analyzed separately for female offspring (Figure 2B). At 3 and 4 weeks of age, the female progeny of the TP group had lower ($P < 0.001$) body weight compared with C and SP groups.

Ovarian follicular populations

There were no significant differences in ovarian follicular numbers between F1 females exposed to HS during embryonic (FP and TP) and fetal (SP and TP) development and their control counterparts (Figure 3). However, there was a significant reduction in the number of primordial follicles in FP compared with both SP and TP groups ($P < 0.05$). In addition, the follicular activation rate was greater ($P < 0.05$) in FP compared with TP females.

Superovulatory responses and gene expression in ovarian tissue of F1 females, and gene expression in F2 blastocysts

The mean number of all recovered structures did not vary significantly among the treatment and control groups in this study (Table 3). The mean number of viable embryos was lower ($P < 0.05$) in TP compared with C group, but it did not differ ($P > 0.05$) among TP and the other HS groups. The ovarian expression of angiotensin 2 receptor (AT2R), as well as the abundance of *ATG8*, *HSP70* (*HSPA1A* and *HSPA1B*), and *HSP60* transcripts, were all greater ($P < 0.05$) in FP, SP, and TP groups compared with C animals (Figure 4). Moreover, the expression of *HSPA1A* was greater ($P < 0.05$) for TP compared with C and SP. The expression of the pro-apoptotic gene *BAX* was greater ($P < 0.05$) in TP and SP compared with controls, and it was lowest for FP group; the opposite behavior was observed in relation to the C group ($P < 0.05$). The abundance of *ATR2*, *HSPA1A*, and *ATG8* transcripts in blastocysts obtained from

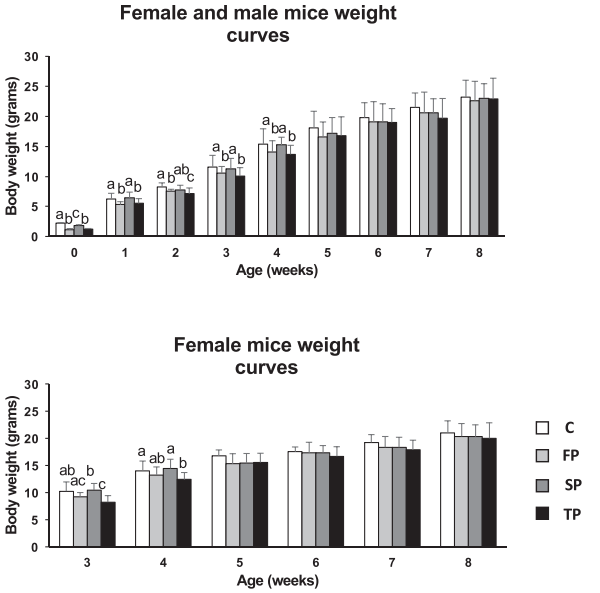

Figure 2. Somatic development (body weight curves) of male and female offspring (A; $n = 155$) and of female offspring only (B; $n = 76$) obtained from C57BL/6 mice exposed to HS during pregnancy. C: control—animals maintained under normothermic conditions; FP—animals subjected to HS daily for 2 h during the first half of pregnancy (days 1–10); SP—animals subjected to HS daily for 2 h during the second half of pregnancy (day 11 to parturition); TP—animals subjected to heat stress daily for 2 h throughout the entire gestational period. Different letters indicate statistical difference ($P < 0.05$) between groups.

superovulated F1 female mice was greater ($P < 0.05$), but the expression of *OCT-4* was lower ($P < 0.05$) for all groups exposed to HS compared with control animals (Figure 5). Furthermore, the expression of *OCT-4* was greater ($P < 0.05$) in SP than in FP and TP groups, and the expression of *HSPA1A* was greater ($P < 0.05$) for TP compared with FP and SP blastocysts.

Discussion

Some evidence from the available literature suggests that HS caused in utero by episodes of heat, whose frequency, intensity, and duration increase each year, have teratogenic effects. Furthermore, it can program a molecular response to HS that is passed onto future generations. However, it is not clear at what stage during the intrauterine development HS induces this new molecular programming response. Hence, in the present study, we assessed the impact of HS at different gestational periods on intrauterine and postnatal development, ovarian follicular populations, and

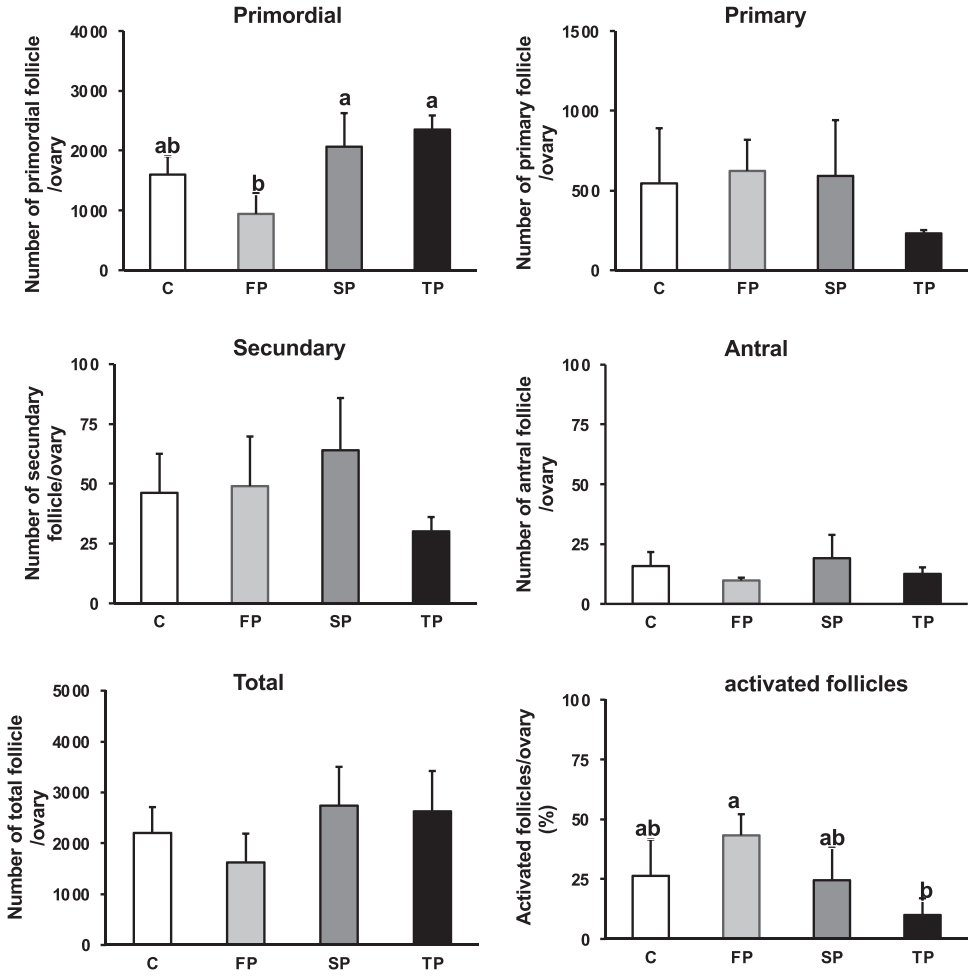

Figure 3. Quantification of ovarian follicular populations in F1 female progeny of C57BL/6 mice ($n = 5$ per group) exposed to HS during different stages of the gestational period. C: control—animals maintained under normothermic conditions; FP—animals subjected to HS daily for 2 h during the first half of pregnancy (days 1–10); SP—animals subjected to HS daily for 2 h during the second half of pregnancy (day 11 to parturition); TP—animals subjected to heat stress daily for 2 h throughout the entire gestational period. Different letters indicate statistical difference ($P < 0.05$) among groups.

Table 3. Superovulatory responses (mean ± SEM) of F1 female mice that received 5 IU of eCG and 5 IU of hCG, respectively, at the 48-h interval.

Groups	Total structures recovered	Viable structures*	Unfertilized eggs	Degenerated embryos
C ($n = 10$)	11.8 ± 5.0	9.5 ± 4.6[a]	1.6 ± 2.0	0.7 ± 0.9
FP ($n = 10$)	7.6 ± 2.4	5.8 ± 2.4[ab]	0.9 ± 1.0	0.7 ± 0.9
SP ($n = 10$)	10.8 ± 5.5	8.1 ± 4.3[ab]	1.0 ± 1.0	2.3 ± 1.6
TP ($n = 10$)	6.9 ± 3.1	4.3 ± 2.7[b]	0.7 ± 0.9	1.9 ± 1.9

C: control—animals maintained under normothermic conditions; FP—animals exposed to heat stress daily for 2 h during the first half of pregnancy (days 1–10); SP—animals exposed to heat stress daily for 2 h during the second half of pregnancy (days 11 to parturition); TP: animals exposed to heat stress daily for 2 h throughout the entire gestational period. *Compact morulae and blastocysts (grades I and II) were considered viable structures. Different letter superscripts in the same column indicate significant differences between groups ($P < 0.05$).

responsiveness to hormonal superovulation, as well as cellular response to HS and its transmission to the next (F2) generation of female mice. The present results indicate that the intrauterine development of the mouse is compromised by exposure to HS during both the embryonic and fetal stages. These findings agree with previous results by Mayvaneh et al. [34] who demonstrated that the exposure of pregnant mice to supraoptimal temperatures (40 and 42°C) daily for 1 h reduced placental weight and diameter as well as the birth-weight of offspring. Padmanabhan et al. [55] observed similar implications of HS in rats after only a single exposure to 41 or 42°C for 1 h on the 9th day of pregnancy. Impeded formation and growth of the placenta lead to diminished placental blood perfusion, which compromises the maternal–fetal gas exchange and transport of nutrients [56]. Protracted concentrations of corticosterone at the end of pregnancy in rats invariably result in low birthweights of offspring [57]. In addition, pregnant females subjected to HS show a reduction in the quantity of food consumed, which consequently flattens their weight gain curve and may result in fetal malnutrition [58]. To recapitulate, there is sufficient evidence in the available literature to support the notion that HS is responsible for the impairment of intrauterine growth in a wide variety of animal species, with more pronounced effects observed in the

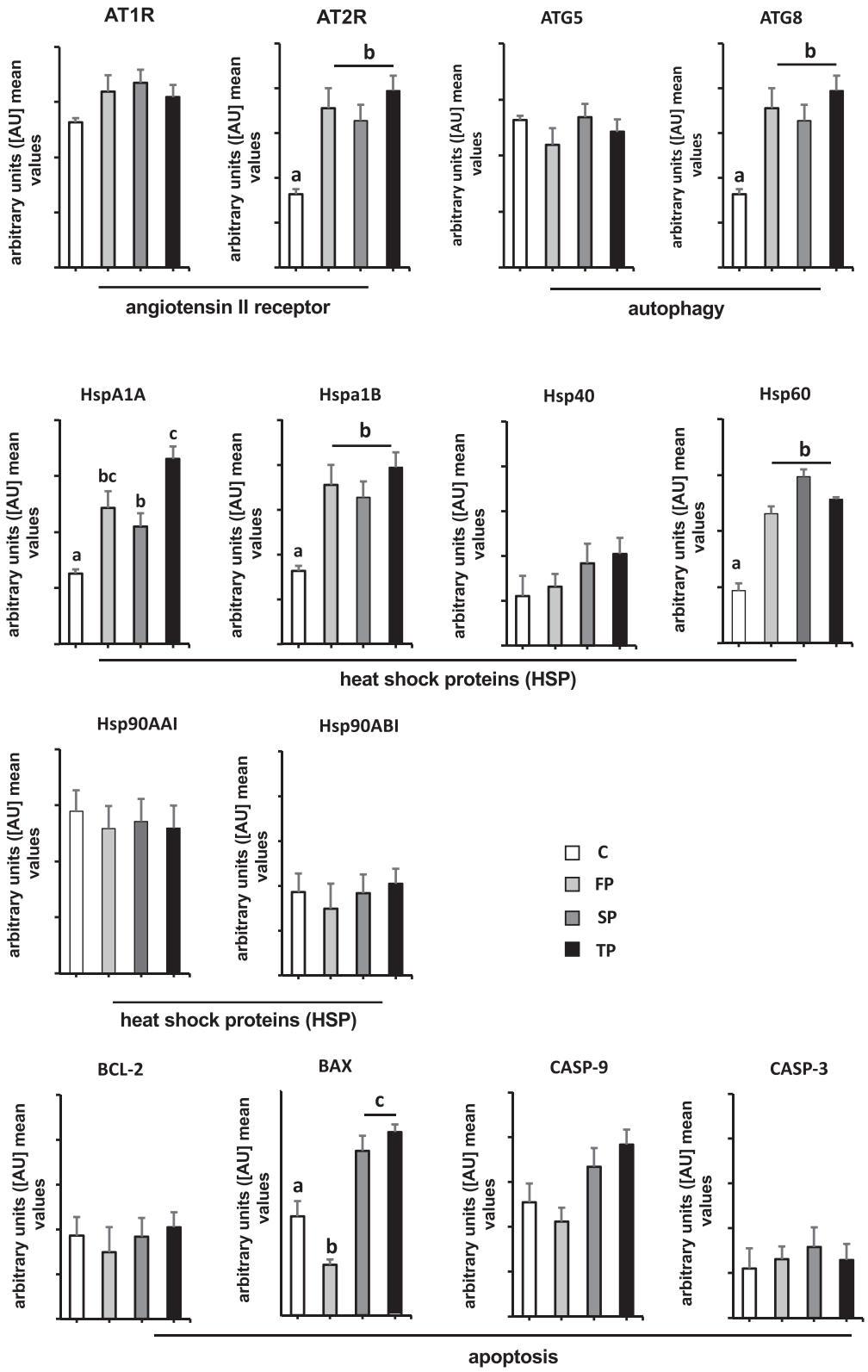

Figure 4. Gene expression in ovarian tissue of F1 female mice. C: control—animals maintained under normothermic conditions; FP—animals subjected to HS daily for 2 h during the first half of pregnancy (days 1–10); SP—animals subjected to HS daily for 2 h during the second half of pregnancy (day 11 to parturition); TP—animals subjected to heat stress daily for 2 h throughout the entire gestational period. Different letters indicate statistical difference ($P < 0.05$) among groups.

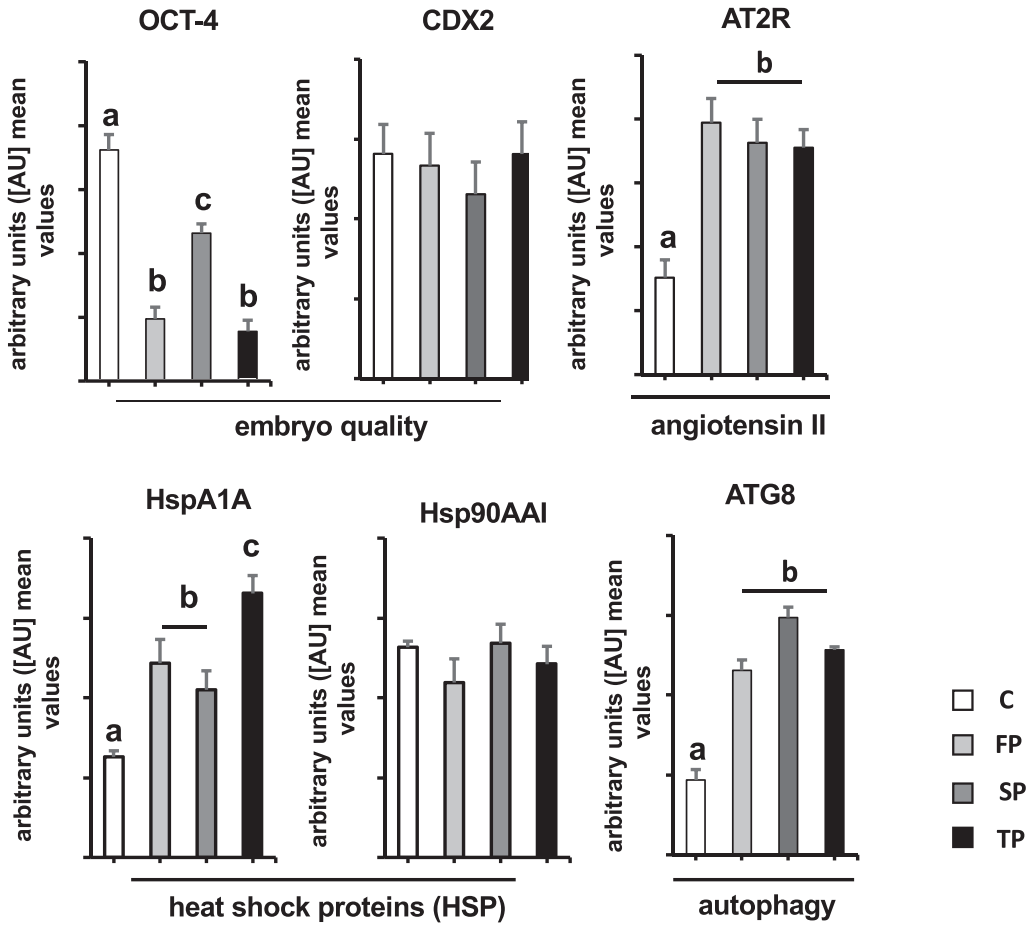

Figure 5. Transcript abundance determined in blastocysts recovered from superovulated F1 females. C: control—animals maintained under normothermic conditions; FP—animals subjected to HS daily for 2 h during the first half of pregnancy (days 1–10); SP—animals subjected to HS daily for 2 h during the second half of pregnancy (day 11 to parturition); TP—animals subjected to heat stress daily for 2 h throughout the entire gestational period. Different letters indicate statistical difference ($P < 0.05$) among groups.

first half of pregnancy, possibly due to hampered placental angiogenesis [59].

Although the mean birthweight was significantly reduced in the mice of the present study, HS did not compromise the survival of pups prior to weaning. Postnatal somatic development (i.e., growth rates) of male and female offspring did not vary among the experimental groups of mice up until the 4th week after birth, as evidenced by the maintenance of differences in mean body weights during that period. Thus, it can also be deduced that HS during the gestational period did not affect the production and quality of milk by lactating females. A similar result was reported by Johnson et al. [58] in rats, exposed to a fluctuating temperate cycle of 30°C daytime and 34°C nighttime, between days 3 and 18 of gestation. Ensuing recovery from intrauterine underdevelopment of animals exposed to HS (from the 5th week of age onwards) suggests a greater capacity for somatic development in these animals, possibly due to an increase in food ingestion and/or conversion capacity. Boddicker et al. [60] reported higher feed intake by fattener pigs from sows subjected to HS during the first half of pregnancy, which resulted in increased fat deposition accompanied by elevated blood concentrations of insulin. In addition, several studies have reported a potential link between HS during pregnancy and increased insulin resistance in the offspring [61], leading to obesity [62]. However, we cannot rule out the possibility that HS-induced molecular changes could increase the conversion of feed into body mass, despite the impairment in milk production. Berghänel et al. [63] demonstrated that prenatal stress accelerated the growth of offspring to compensate for the reduced maternal investment in mammals.

In the present study, no differences were found in the number of ovarian follicles between the offspring submitted to HS in utero compared with control animals; however, the number of primordial follicles in FP was lower compared with that in SP and TP groups. Autophagy functions as an important mechanism responsible for maintaining the survival of primordial germ cells during the postpartum period of mice [64]. Watanabe et al. [65] reported that autophagy in neonatal mice increased the pool of primordial follicles and improved fertility by extending the reproductive lifespan of females. Based on these observations, it is logical to suggest that the greater number of primordial follicles in SP and TP groups compared with FP mice may be in part due to the upregulation of HS-mediated autophagy in the final stage of pregnancy. Naturally, the population of primordial follicles undergoes a

significant reduction during the postpartum period of mice [66]. Stress triggered by the shift from placental to lactational nutrition is one of the most likely causes of this depletion in a pool of primordial ovarian follicles [67]. It is attractive to speculate that individuals exposed to HS in the final period of pregnancy may be better adapted to or "prepared for" the stress of the "nutritional and environmental switch" than animals affected by HS early in gestation. The underlying mechanism(s) of such differences remain to be elucidated.

There was a reciprocal relationship between primordial follicle numbers and follicular activation in FP and TP groups; FP mice showed a simultaneous reduction in the number of primordial follicles and an increase in follicular activation, whereas TP mice showed an increase in the number of primordial follicles and a reduction in follicular activation. Specific reasons for these results remain uncertain. However, Gaytan et al. [68] suggested that the rate of follicular recruitment could be determined by the differences in the ovarian microenvironment, and specifically in the degree of follicular "crowding." The clusters of preantral follicles generate inhibitory signals that locally suppress the activation of adjacent follicles. Hence, an increase in the number of primordial follicles would result in a greater follicular aggregation and, consequently, a lower rate of follicle recruitment and vice versa; any condition resulting in a reduction of primordial follicle numbers and agglomeration would boost follicular activation rates. In the present study, there were no significant differences in the mean number of primary, secondary, and antral follicles between the four experimental groups, indicating that HS had a limited effect on the viability of activated ovarian follicles.

Lower production of viable embryos in the TP group (exposed to HS for the longest time) may be associated with impaired functioning of the hypothalamic–pituitary–gonadal axis. According to Dantzer and Mormede [69], prolonged stress can negatively affect the functioning of the hypothalamic–pituitary–gonadal axis and consequently compromise the reproductive processes. Antral follicular growth and steroidogenesis, manifestation of sexual behavior, ovulation, and embryo implantation are the most sensitive reproductive processes that can be altered by stress, as they are largely governed by the neuroendocrine system [70]. Mechanistic studies suggest that HS decreases the secretion of gonadotropic hormones [71], in addition to down-regulating the expression of gonadotropic receptors and pregnenolone biosynthesis due to inhibition of the cytochrome P450 side-chain cleavage (P450scc) activity [72].

Exposure of developing embryos and fetuses to insults such as HS can induce molecular, structural, and functional changes that persist during the postnatal period [73] and can ultimately be transferred to offspring [74]. To investigate the molecular aspects of this prenatal reprogramming, we evaluated the expression of several genes that can potentially be affected by HS in ovarian tissue and embryos. The HS response is highly conserved and is associated with the expression of several inducible proteins called heat shock proteins (HSPs). Angiotensin II induces HSP expression in the aorta and kidney, and cultured smooth muscle cells [25]. In the present experiment, increased expression of angiotensin II type 2 receptors (*AT2R*) was observed in the ovary of mice subjected to HS and in their progeny; this might increase cellular sensitivity to angiotensin II (and possibly other ligands) and consequently contribute to an increase in *HSP* expression. In addition, AT2R receptors are involved in peripheral vasodilation, which may play a vital role during thermoregulation [12]. All these changes appear to be indicative of adaptations to a hot environment. However, these adaptations in developing blastocysts appear to occur simultaneously with some negative alterations in metabolic pathways, as evidenced by a decline in *OCT-4* gene expression, especially in the embryos from mice exposed to HS during the first half of gestation (both FP and TP). The OCT4 is a core transcription factor involved in the maintenance of pluripotency in the early mammalian embryo [75]. The *ATG8* gene expression was increased in the ovarian tissue of female mice subjected to HS in prenatal life and in the embryos which they produced following superovulation. According to Li et al. [76], the activation of autophagy by HS involves the phosphorylation of calcium channels in the endoplasmic reticulum and ensuing release of Ca^{2+} to cell cytosol. Elevated concentrations of Ca^{2+} in the cytoplasm stimulate autophagosome maturation via a process mediated by ATG8 [77]. Thus, an increase in *ATG8* expression may contribute to the recycling of organelles compromised by stress.

In conclusion, our results indicate that maternal exposure to HS negatively affected the intrauterine development of the offspring. This effect was more pronounced when exposure to HS occurred during the first half of pregnancy. Moreover, HS exerted a negative effect on the somatic development of offspring in FP and TP females. In addition, the expression of genes involved in the physiological (*AT2R*) and cellular response to HS (*HSPA1A*; *HSPA1B*; *HSP60*; *HSP90A*), elimination of macromolecules and organelles damaged by autophagy (*ATG8*), and programmed cell death (*BAX*) was affected in F1 mice regardless of the timing and duration of gestational HS. The ability of F1 mice to transmit those changes in *AT2R*, *HSPA1A*, and *ATG8 e*xpression profiles was confirmed in F2 embryos. However, a decrease in the expression of the *OCT-4* gene in the blastocysts derived from F1 mice may suggest the occurrence of compromised embryonic viability, especially in FP and TP groups. Collectively, the present results indicate that HS can significantly alter prenatal development in mice with the carry-over effects manifest in the reproductive organs of female progeny (F1 generation) and the blastocysts they produce (F2 generation).

Acknowledgment

The authors thank the Universidade Federal Fluminense, Conselho Nacional de Desenvolvimento Científico e Tecnológico (CNPq). JMGS-F is a fellow of FAPERJ and CNPq.

Author contributions

JRS—data analysis and manuscript writing; JMGS-F—design of the project, data analysis, and manuscript writing; TFMB—data analysis; JRS—data collection and analysis; CRFM—data collection and analysis; PMB—manuscript writing and editing; RITPB—design of the project, data collection and analysis, and manuscript writing and editing.

Conflict of Interest

The authors have declared that no conflict of interest exists.

Data availability

The data underlying this article may be shared upon reasonable request to the corresponding author.

References

1. Romanello M, Di Napoli C, Drummond P, *et al.* The 2022 report of the *Lancet* Countdown on health and climate change: health at the mercy of fossil fuels. *Lancet* 2022; **400**:1619–1654.
2. Masson-Delmotte VP, Zhai A, Pirani SL, *et al.* (eds.). Intergovernmental panel on climate change. In: *Climate Change 2021: The Physical Science Basis. Working Group I Contribution to the IPCC Sixth Assessment Report*. Cambridge and New York, NY: Cambridge University Press; 2021.
3. Turek-Hankins LL, Perez EC, Scarpa G, *et al.* Climate change adaptation to extreme heat: a global systematic review of implemented action. *Oxf Open Clim Chang* 2021; **1**:kgab005.
4. Ren C, Williams GM, Tong S. Does particulate matter modify the association between temperature and cardiorespiratory diseases? *Environ Health Perspect* 2006; **114**:1690–1696.
5. Robine JM, Cheung SL, Le Roy S, *et al.* Death toll exceeded 70,000 in Europe during the summer of 2003. *C R Biol* 2008; **331**: 171–178.
6. West JW. Nutritional strategies for managing the heat-stressed dairy cow. *J Dairy Sci* 1999; **2**:21–35.
7. Boni R. Heat stress, a serious threat to reproductive function in animals and humans. *Mol Reprod Dev* 2019; **86**:1307–1323.
8. Kenny GP, Jay O. Thermometry, calorimetry, and mean body temperature during heat stress. *Compr Physiol* 2013; **3**: 1689–1719.
9. González-Alonso J, Mora-Rodríguez R, Below P, *et al.* Dehydration markedly impairs cardiovascular function in hyperthermic endurance athletes during exercise. *J Appl Physiol* 1985; **82**: 1229–1236.
10. Roncal-Jimenez C, Lanaspa M, Jensen T, Sanchez-Lozada LG, Johnson RJ. Mechanisms by which dehydration may lead to chronic kidney disease. *Ann Nutr Metab* 2015; **66**:10–13.
11. Glaser J, Lemery J, Rajagopalan B, Diaz HF, García-Trabanino R, Taduri G, Madero M, Amarasinghe M, Abraham G, Anutrakulchai S, Jha V, Stenvinkel P, *et al.* Climate change and the emergent epidemic of CKD from heat stress in rural communities: the case for heat stress nephropathy. *Clin J Am Soc Nephrol* 2016; **11**: 1472–1483.
12. Chen Y, Ross BM, Currie RW. Heat shock treatment protects against angiotensin II-induced hypertension and inflammation in aorta. *Cell Stress Chaperones* 2004; **9**:99–107.
13. Oh E, Kim JY, Cho Y, An H, Lee N, Jo H, Ban C, Seo JH. Overexpression of angiotensin II type 1 receptor in breast cancer cells induces epithelial-mesenchymal transition and promotes tumor growth and angiogenesis. *Biochim Biophys Acta* 2016; **1863**:1071–1081.
14. Liao X, Xiao J, Li SH, Xiao LL, Cheng B, Fu XB, Cui T, Liu HW. Critical role of the endogenous renin-angiotensin system in maintaining self-renewal and regeneration potential of epidermal stem cells. *Biochim Biophys Acta Mol Basis Dis* 2019; **1865**: 2647–2656.
15. Kuhl NM, Rensing L. Heat shock effects on cell cycle progression. *Cell Mol Life Sci* 2000; **57**:450–463.
16. Parsell DA, Lindquist S. The function of heat-shock proteins in stress tolerance: degradation and reactivation of damaged proteins. *Annu Rev Genet* 1993; **27**:437–496.
17. Sonna LA, Fujita J, Gaffin SL, Lilly CM. Invited Review: Effects of heat and cold stress on mammalian gene expression. *J Appl Physiol* 1985; **92**:1725–1742.
18. Skibiel AL, Peñagaricano F, Amorín R, Ahmed BM, Dahl GE, Laporta J. In utero heat stress alters the offspring epigenome. *Sci Rep* 2018; **8**:14609.
19. Pirkkala L, Nykänen P, Sistonen L. Roles of the heat shock transcription factors in regulation of the heat shock response and beyond. *FASEB J* 2001; **15**:1118–1131.
20. Trinklein ND, Murray JI, Hartman SJ, Botstein D, Myers RM. The role of heat shock transcription factor 1 in the genome-wide regulation of the mammalian heat shock response. *Mol Biol Cell* 2004; **15**:1254–1261.
21. Akerfelt M, Morimoto RI, Sistonen L. Heat shock factors: integrators of cell stress, development and lifespan. *Nat Rev Mol Cell Biol* 2010; **11**:545–555.
22. Welch WJ. Mammalian stress response: cell physiology, structure/function of stress proteins, and implications for medicine and disease. *Physiol Rev* 1992; **72**:1063–1081.
23. Currie RW. Plumier J-CL The heat shock response and tissue protection. In: Baxter GF, Yellon DM (eds.), *Delayed Preconditioning and Adaptive Cardioprotection*. Dordrecht: Kluwer Academic Publishers; 1998: 135–153.
24. Krueger-Naug AM, Plumier JC, Hopkins DA, *et al.* HSP27 in the nervous system: expression in pathophysiology and in the aging brain. *Prog Mol Subcell Biol* 2002; **28**:235–251.
25. Ishizaka N, Aizawa T, Ohno M, Usui SI, Mori I, Tang SS, Ingelfinger JR, Kimura S, Nagai R. Regulation and localization of HSP70 and HSP25 in the kidney of rats undergoing long-term administration of angiotensin II. *Hypertension* 2002; **39**:122–128.
26. Cuervo AM. Autophagy and aging: keeping that old broom working. *Trends Genet* 2008; **24**:604–612.
27. Tan H, Huang F, Huang M, Wu X, Tong Z. HSF1 attenuates the release of inflammatory cytokines induced by lipopolysaccharide through transcriptional regulation of Atg10. *Microbiol Spectr* 2023; **11**:e0305922.
28. Tamura Y, Matsunaga Y, Kitaoka Y, Hatta H. Effects of heat stress treatment on age-dependent unfolded protein response in different types of skeletal muscle. *J Gerontol A Biol Sci Med Sci* 2017; **72**: 299–308.
29. Palikaras K, Lionaki E, Tavernarakis N. Mechanisms of mitophagy in cellular homeostasis, physiology and pathology. *Nat Cell Biol* 2018; **20**:1013–1022.
30. Pyo JO, Yoo SM, Ahn HH, Nah J, Hong SH, Kam TI, Jung S, Jung YK. Overexpression of Atg5 in mice activates autophagy and extends lifespan. *Nat Commun* 2013; **4**:2300.
31. Lee SE, Hwang KC, Sun SC, Xu YN, Kim NH. Modulation of autophagy influences development and apoptosis in mouse embryos developing in vitro. *Mol Reprod Dev* 2011; **78**:498–509.
32. D'Amato G, Chong-Neto HJ, Monge Ortega OP, *et al.* The effects of climate change on respiratory allergy and asthma induced by pollen and mold allergens. *Allergy* 2020; **75**:2219–2228.
33. Balbus JM, Malina C. Identifying vulnerable subpopulations for climate change health effects in the United States. *J Occup Environ Med* 2009; **51**:33–37.
34. Mayvaneh F, Entezari A, Sadeghifar F, Baaghideh M, Guo Y, Atabati A, Zhao Q, Zhang Y. Exposure to suboptimal ambient temperature during specific gestational periods and adverse outcomes in mice. *Environ Sci Pollut Res Int* 2020; **27**:45487–45498.
35. McElroy S, Ilango S, Dimitrova A, Gershunov A, Benmarhnia T. Extreme heat, preterm birth, and stillbirth: a global analysis across 14 lower-middle income countries. *Environ Int* 2022; **158**:106902.
36. Syed S, O'Sullivan TL, Phillips KP. Extreme heat and pregnancy outcomes: a scoping review of the epidemiological evidence. *Int J Environ Res Public Health* 2022; **19**:2412.
37. Carolan-Olah M, Frankowska D. High environmental temperature and preterm birth: a review of the evidence. *Midwifery* 2014; **30**: 50–59.
38. Kuehn L, McCormick S. Heat exposure and maternal health in the face of climate change. *Int J Environ Res Public Health* 2017; **14**:853.
39. Chersich MF, Pham MD, Areal A, Haghighi MM, Manyuchi A, Swift CP, Wernecke B, Robinson M, Hetem R, Boeckmann M, Hajat S. Associations between high temperatures in pregnancy and

risk of preterm birth, low birth weight, and stillbirths: systematic review and meta-analysis. *BMJ* 2020; **371**:m3811.
40. Aroyo A, Yavin S, Arav A, Roth Z. Maternal hyperthermia disrupts developmental competence of follicle-enclosed oocytes: in vivo and ex vivo studies in mice. *Theriogenology* 2007; **67**:1013–1021.
41. Batista RI, Wohlres-Viana S, Pinto IS, Maffili VV, Viana JHM. Somatic development and embryo yield in crossbred F1 mice generated by different mating strategies. *Braz J Biol* 2010; **70**: 145–149.
42. García-Vargas D, Juárez-Rojas L, Rojas Maya S, Retana-Márquez S. Prenatal stress decreases sperm quality, mature follicles and fertility in rats. *Syst Biol Reprod Med* 2019; **65**:223–235.
43. Campos-Junior PH, Assunção CM, Carvalho BC, *et al.* Follicular populations, recruitment and atresia in the ovaries of different strains of mice. *Reprod Biol* 2012; **12**:41–55.
44. Gougeon A, Chainy GB. Morphometric studies of small follicles in ovaries of women at different ages. *J Reprod Fertil* 1987; **81**: 433–442.
45. Pfaffl MW, Tichopad A, Prgomet C, Neuvians TP. Determination of stable housekeeping genes, differentially regulated target genes and sample integrity: BestKeeper–Excel-based tool using pair-wise correlations. *Biotechnol Lett* 2004; **26**:509–15.
46. Zhang XF, Park JH, Choi YJ, Kang MH, Gurunathan S, Kim JH. Silver nanoparticles cause complications in pregnant mice. *Int J Nanomedicine* 2015; **10**:7057–7071.
47. Huang Q, Xiong H, Yang H, Ou Y, Zhang Z, Chen S, Ye Y, Zheng Y. Differential expression of Bcl-2 in the cochlea and auditory cortex of a mouse model of age-related hearing loss. *Audiol Neurootol* 2016; **21**:326–332.
48. Qiao N, Chen H, Du P, *et al.* Acetyl-L-carnitine induces autophagy to promote mouse spermatogonia cell recovery after heat stress damage. *Biomed Res Int* 2021; **2021**:1–11.
49. Zhu Y, Zhu J, Wan X, Zhu Y, Zhang T. Gene expression of sHsps, Hsp40 and Hsp60 families in normal and abnormal embryonic development of mouse forelimbs. *Toxicol Lett* 2010; **193**:242–251.
50. Zhu Y, Ren C, Wan X, Zhu Y, Zhu J, Zhou H, Zhang T. Gene expression of Hsp70, Hsp90 and Hsp110 families in normal palate and cleft palate during mouse embryogenesis. *Toxicol Ind Health* 2013; **29**:915–930.
51. Xiao L, Song Y, Huang W, Yang S, Fu J, Feng X, Zhou M. Expression of SOX2, NANOG and OCT4 in a mouse model of lipopolysaccharide-induced acute uterine injury and intrauterine adhesions. *Reprod Biol Endocrinol* 2017; **15**:14.
52. Bhusari S, Hearne LB, Spiers DE, Lamberson WR, Antoniou E. Transcriptional profiling of mouse liver in response to chronic heat stress. *J Therm Biol* 2008; **33**:157–167.
53. Ruiz-Villalba A, Mattiotti A, Gunst QD, Cano-Ballesteros S, van den Hoff MJB, Ruijter JM. Reference genes for gene expression studies in the mouse heart. *Sci Rep* 2017; **7**:24.
54. Yu L, Shao C, Gao L. Developmental expression patterns for angiotensin receptors in mouse skin and brain. *J Renin Angiotensin Aldosterone Syst* 2014; **15**:139–149.
55. Padmanabhan R, Al-Menhali NM, Ahmed I, *et al.* Histological, histochemical and electron microscopic changes of the placenta induced by maternal exposure to hyperthermia in the rat. *Int J Hyperthermia* 2005; **21**:29–44.
56. Akbarinejad V, Gharagozlou F, Vojgani M. Temporal effect of maternal heat stress during gestation on the fertility and anti-Müllerian hormone concentration of offspring in bovine. *Theriogenology* 2017; **99**:69–78.
57. Cheong JN, Cuffe JS, Jefferies AJ, Anevska K, Moritz KM, Wlodek ME. Sex-specific metabolic outcomes in offspring of female rats born small or exposed to stress during pregnancy. *Endocrinology* 2016; **157**:4104–4120.
58. Johnson JS, Abuajamieh M, Victoria Sanz Fernandez M, Seibert JT, Stoakes SK, Keating AF, Ross JW, Selsby JT, Rhoads RP, Baumgard LH. The impact of in utero heat stress and nutrient restriction on progeny body composition. *J Therm Biol* 2015; **53**:143–150.
59. Ozawa M, Hirabayashi M, Kanai Y. Developmental competence and oxidative state of mouse zygotes heat-stressed maternally or in vitro. *Reproduction* 2002; **124**:683–689.
60. Boddicker RL, Seibert JT, Johnson JS, Pearce SC, Selsby JT, Gabler NK, Lucy MC, Safranski TJ, Rhoads RP, Baumgard LH, Ross JW. Gestational heat stress alters postnatal offspring body composition indices and metabolic parameters in pigs. *PloS One* 2014; **9**:e110859.
61. Wan X, He X, Liu Q, Wang X, Ding X, Li H. Frequent and mild scrotal heat stress in mice epigenetically alters glucose metabolism in the male offspring. *Am J Physiol Endocrinol Metab* 2020; **319**:E291–E304.
62. Johnson JS, Stewart KR, Safranski TJ, Ross JW, Baumgard LH. In utero heat stress alters postnatal phenotypes in swine. *Theriogenology* 2020; **154**:110–119.
63. Berghänel A, Heistermann M, Schülke O, Ostner J. Prenatal stress accelerates offspring growth to compensate for reduced maternal investment across mammals. *Proc Natl Acad Sci U S A* 2017; **114**:E10658–E10666.
64. Rodrigues P, Limback D, McGinnis LK, Plancha CE, Albertini DF. Multiple mechanisms of germ cell loss in the perinatal mouse ovary. *Reproduction* 2009; **137**:709–720.
65. Watanabe R, Sasaki S, Kimura N. Activation of autophagy in early neonatal mice increases primordial follicle number and improves lifelong fertility†. *Biol Reprod* 2020; **102**:399–411.
66. Faire M, Skillern A, Arora R, Nguyen DH, Wang J, Chamberlain C, German MS, Fung JC, Laird DJ. Follicle dynamics and global organization in the intact mouse ovary. *Dev Biol* 2015; **403**: 69–79.
67. Sun YC, Wang YY, Sun XF, Cheng SF, Li L, Zhao Y, Shen W, Chen H. The role of autophagy during murine primordial follicle assembly. *Aging (Albany NY)* 2018; **10**:197–211.
68. Gaytan F, Morales C, Leon S, Garcia-Galiano D, Roa J, Tena-Sempere M. Crowding and follicular fate: spatial determinants of follicular reserve and activation of follicular growth in the mammalian ovary. *PloS One* 2015; **10**:e0144099.
69. Dantzer R, Mormède P. Stress in farm animals: a need for reevaluation. *J Anim Sci* 1983; **57**:6–18.
70. Einarsson S, Brandt Y, Lundeheim N, Madej A. Stress and its influence on reproduction in pigs: a review. *Acta Vet Scand* 2008; **50**:48.
71. Schoonmaker JN, Erickson GF. Glucocorticoid modulation of follicle-stimulating hormone-mediated granulosa cell differentiation. *Endocrinology* 1983; **113**:1356–1363.
72. Tilbrook AJ, Turner AI, Clarke IJ. Effects of stress on reproduction in non-rodent mammals: the role of glucocorticoids and sex differences. *Rev Reprod* 2000; **5**:105–113.
73. Lindström J. Early development and fitness in birds and mammals. *Trends Ecol Evol* 1999; **14**:343–348.
74. Sharma U, Conine CC, Shea JM, Boskovic A, Derr AG, Bing XY, Belleannee C, Kucukural A, Serra RW, Sun F, Song L, Carone BR, *et al.* Biogenesis and function of tRNA fragments during sperm maturation and fertilization in mammals. *Science* 2016; **351**: 391–396.
75. Hisey E, Ross PJ, Meyers SA. A review of OCT4 functions and applications to equine embryos. *J Equine Vet Sci* 2021; **98**: 103364.
76. Li L, Tan H, Gu Z, Liu Z, Geng Y, Liu Y, Tong H, Tang Y, Qiu J, Su L. Heat stress induces apoptosis through a Ca^{2+}-mediated mitochondrial apoptotic pathway in human umbilical vein endothelial cells. *PloS One* 2014; **9**:e111083.
77. Choi S, Kim HJ. The Ca2+ channel TRPML3 specifically interacts with the mammalian ATG8 homologue GATE16 to regulate autophagy. *Biochem Biophys Res Commun* 2014; **443**:56–61.